Preferential associations between co-regulated genes reveal a transcriptional interactome in erythroid cells

Stefan Schoenfelder[1,6], Tom Sexton[1,5,6], Lyubomira Chakalova[1,5,6], Nathan F Cope[1], Alice Horton[1], Simon Andrews[2], Sreenivasulu Kurukuti[1,5], Jennifer A Mitchell[1,5], David Umlauf[1,5], Daniela S Dimitrova[1], Christopher H Eskiw[1], Yanquan Luo[3], Chia-Lin Wei[3], Yijun Ruan[3], James J Bieker[4] & Peter Fraser[1]

The discovery of interchromosomal interactions in higher eukaryotes points to a functional interplay between genome architecture and gene expression, challenging the view of transcription as a one-dimensional process. However, the extent of interchromosomal interactions and the underlying mechanisms are unknown. Here we present the first genome-wide analysis of transcriptional interactions using the mouse globin genes in erythroid tissues. Our results show that the active globin genes associate with hundreds of other transcribed genes, revealing extensive and preferential intra- and interchromosomal transcription interactomes. We show that the transcription factor Klf1 mediates preferential co-associations of Klf1-regulated genes at a limited number of specialized transcription factories. Our results establish a new gene expression paradigm, implying that active co-regulated genes and their regulatory factors cooperate to create specialized nuclear hot spots optimized for efficient and coordinated transcriptional control.

Increasing evidence suggests that long-range interactions between genomic regions contribute to the regulation of gene expression[1]. In higher eukaryotes individual chromosomes occupy discrete chromosome territories in the three-dimensional space of the nucleus[2]. However, chromosomal regions often loop out of their chromosome territories in association with activation[3,4], and neighboring chromosomes can intermingle[5], resulting in potentially functional contacts between genomic regions located on different chromosomes. Indeed, examples of interchromosomal interactions that regulate gene expression have been described[6–8].

Genomic regions dynamically relocate to specialized subnuclear compartments that favor gene activation or silencing[9–11]. For example, RNA polymerase II (RNAPII) transcription occurs at transcription factories[12–16], subnuclear compartments that are highly enriched in the active, hyperphosphorylated forms of RNAPII[17]. Transcription of most 'active' genes is not continuous but occurs in pulses of activity[10,14,18–20]. Gene activation is associated with relocation of genes to transcription factories[13–15], indicating that transcriptional pulses occur by virtue of dynamic associations with transcription factories[10]. Previous studies on a limited number of transcriptionally active genes revealed long-range intra- and interchromosomal gene associations at shared transcription factories[10,14]. However, the extent and nature of these transcriptional associations is unclear, as is the question of whether they contribute to the control of gene expression.

Here we present a genome-wide analysis of gene co-associations in transcription factories with the mouse *Hbb* and *Hba* globin genes, using a new variant of the 3C technique[21] combined with chromatin immunoprecipitation (ChIP). The results are corroborated by extensive FISH and immunofluorescence analyses of transcriptional co-associations at transcription factories. Collectively, our results show that co-regulated genes preferentially cluster at specialized transcription factories that seem to be optimized for their high-level transcription.

RESULTS

Preferential interchromosomal associations at factories

We used triple-label RNA immuno-FISH to examine interchromosomal associations between transcriptionally active genes at transcription factories. We chose five erythroid-expressed genes and analyzed their subnuclear location relative to transcription factories and the constitutively transcribed *Hba* and *Hbb* genes (**Fig. 1a**). In agreement with previous studies[10,14,15], we found that the vast majority of RNA FISH signals (93–99%) overlapped with RNAPII foci (**Fig. 1b**). Furthermore, we found that essentially all colocalizing (overlapping) RNA FISH signals were localized to the same RNAPII focus (97–100%) (**Fig. 1c**). These data confirm earlier results[10,12,15–17] indicating that virtually all gene transcription occurs at transcription factories. We conclude that overlapping RNA FISH signals are an excellent indicator of genes sharing the same transcription factory.

[1]Laboratory of Chromatin and Gene Expression and [2]Bioinformatics Group, The Babraham Institute, Babraham Research Campus, Cambridge, UK. [3]Genome Institute of Singapore, Singapore, Singapore. [4]Department of Developmental and Regenerative Biology, Mount Sinai School of Medicine, New York, New York, USA. [5]Current addresses: Institute of Human Genetics, Montpellier Cedex 5, France (T.S.); Research Centre for Genetic Engineering and Biotechnology, Macedonian Academy of Sciences and Arts, Skopje, Republic of Macedonia (L.C.); Division of Cancer Sciences and Molecular Pathology, Section of Pathology and Gene Regulation, University of Glasgow, Glasgow, UK (S.K.); Department of Cell and Systems Biology, University of Toronto, Toronto, Ontario, Canada (J.A.M.); Institute of Genetics and Molecular Cell Biology, Illkirch Cedex, France (D.U.). [6]These authors contributed equally to this work. Correspondence should be addressed to P.F. (peter.fraser@bbsrc.ac.uk).
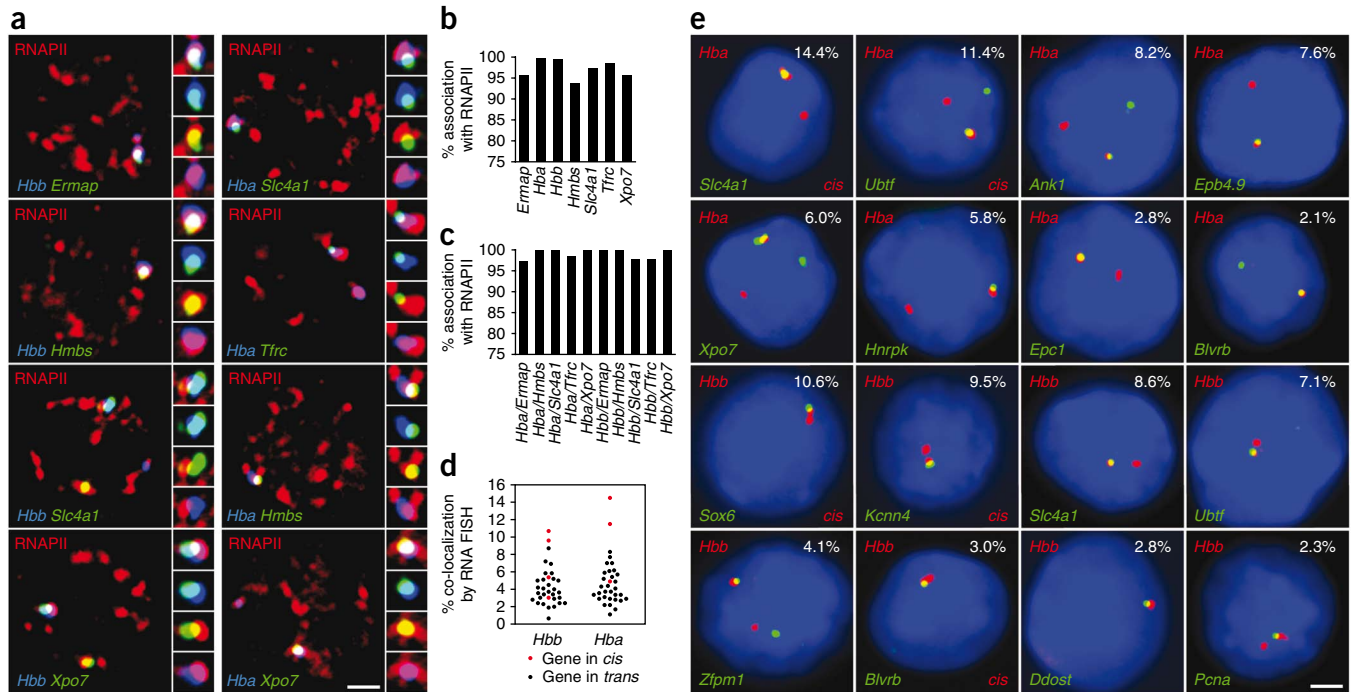
Figure 1 Genes interchromosomally co-associate in transcription factories. (**a**) Triple-label RNA immuno-FISH of gene pairs and RNAPII factories. RNAPII-S5P staining is in red and RNA FISH signals are in green and blue, as indicated, for each gene pair. Side panels show enlarged images of the colocalizing FISH signals (top to bottom: triple label, blue and green, red and green, red and blue). Scale bar, 2 μm. (**b**,**c**) Bar charts showing percentages of RNA FISH signals that associate with an RNAPII factory (**b**) and percentages of colocalizing RNA FISH signals that co-associate within the same RNAPII focus (**c**). (**d**) Scatter plot showing distributions of RNA FISH colocalization frequencies for genes in *cis* (red) and *trans* (black) with *Hba* and *Hbb*. (**e**) Representative double-label RNA FISH in definitive erythroid cells for several erythroid-expressed genes (green) and *Hba* or *Hbb* (red), as indicated, with DAPI staining in blue. Colocalization frequencies are shown on each panel, and co-associations in *cis* are labeled. Scale bar, 2 μm.

Recent reports have noted that active genes up to 1 μm apart frequently associate with the same large nuclear Sc35 speckle domain, with the suggestion that Sc35 domains may spatially organize active genes[22–24]. We found that mouse erythroid cells lack large speckle domains (**Supplementary Note** and **Supplementary Fig. 1a–c**). Furthermore, we found that transcribed genes vary greatly in their frequency of association with Sc35 (**Supplementary Fig. 1d**), in agreement with previous reports[22,23,25,26]. These results argue strongly against a universal role for Sc35 domains in organizing active genes in eukaryotic nuclei.

To obtain a more comprehensive picture of transcriptional co-associations, we used double-label RNA FISH to quantify transcriptional associations between *Hba*, *Hbb* and 33 erythroid-expressed genes, located on 15 mouse chromosomes. We observed a considerable range of interchromosomal colocalization frequencies (up to 17-fold; **Fig. 1d,e**), indicating that genes nonrandomly co-associate with preferential transcription partners in factories (**Supplementary Table 1**). Consistent with previous results[14], linked genes generally co-associated at higher frequencies than genes in *trans*. However, we found that co-association frequencies between some genes in *trans* can surpass those of linked genes (**Fig. 1d** and **Supplementary Table 1**). These findings demonstrate preferential interchromosomal co-associations between specific genes in shared transcription factories.

## Genome-wide detection of transcriptional co-associations
To obtain a global view of the repertoire of transcriptional interactions (the transcriptional interactome) for *Hba* and *Hbb* in erythroid nuclei, we developed e4C (enhanced ChIP-4C), a new genome-wide adaptation of the 4C assay, incorporating two major modifications

(**Fig. 2a**). First, to focus on gene interactions within transcription factories, we included a ChIP step with an antibody recognizing the phosphorylated Ser5 residue of the C-terminal domain (CTD) of the largest subunit of RNA polymerase II (RNAPII-S5P), the form implicated in transcriptional initiation and elongation[27]. Real-time PCR analysis of RNAPII-S5P ChIP DNA showed that active gene sequences were highly enriched (**Fig. 2b**). The immunoprecipitated chromatin was then diluted as for conventional 3C to favor ligation between DNA strands in the same cross-linked complex. Known long-range transcription factory associations between *Hbb* and distal active genes[14] were detected by 3C assays on RNAPII-S5P ChIP material (**Fig. 2c**), demonstrating that the ChIP step maintains associations between genes in shared transcription factories. In contrast, no interaction of *Hbb* with the nearby inactive *P2ry6* gene was detected[14].

Second, we incorporated a pre-enrichment step for bait-linked sequences. This provided a more than 100-fold increase in signal-to-noise ratio, affording the identification of distal *cis*- and *trans*-interacting loci with higher sensitivity and confidence (data not shown). In brief, the pre-enrichment step involves primer extension with a biotinylated bait-specific primer, and specific pulldown of bait-linked 3C products with streptavidin beads, before amplification with a bait-specific, nested primer. Cloning and sequencing of *Hbb* e4C products revealed that 95% (121 of 127) had the expected structure, indicating that e4C is highly efficient (**Fig. 2a**). We then hybridized the e4C DNA to custom microarrays covering most of the nonrepetitive mouse genome (see Online Methods).

Analysis of the microarray data shows that e4C detects known erythroid-specific associations between *Hbb* and the distal transcribed *Ahsp* (formerly *Eraf*) and *Uros* genes[14,28] (**Fig. 2c**), whereas the nearby

Figure 2 e4C detects known and heretofore uncharacterized genomic co-associations with *Hbb* in *cis* and *trans*. (**a**) Overview of the e4C method. Nuclei are cross-linked, and the chromatin is digested with BglII as in conventional 3C, before immunoprecipitation with an antibody recognizing RNAPII-S5P. DNA ligation is performed on the immunoprecipitated chromatin under dilute conditions that favor ligation between DNA strands within cross-linked complexes. After reversal of the cross-links and DNA purification, a biotinylated primer (brown) specific to the bait gene (red) is used for primer extension into adjacent ligation products (blue). Biotinylated extension products are purified on streptavidin-coated magnetic beads (red sphere), digested with NlaIII and ligated to an adaptor (green). e4C products are amplified by PCR with a nested, bait-specific primer (yellow) and an adaptor-specific primer (green). e4C products are then analyzed by cloning and sequencing, or hybridization to a custom microarray. (**b**) Bar chart showing the enrichments of erythroid-expressed *Hba*, *Slc4a1* and *Ahsp* sequences after ChIP using an antibody recognizing RNAPII-S5P. Enrichments of nonexpressed *Nefm* (formerly *Nef3*) and *Igh* V_H16 sequences are shown as negative controls. Enrichments are shown relative to the V_H16 control. (**c**) *Hbb* e4C microarray profiles for three ~2-Mb regions of genomic sequence in *cis* to *Hbb*, centered on *Ahsp*, *Uros* and *P2ry6*, showing the running mean enrichments of e4C signal over genomic signal for 100-kilobase (kb) windows. Black bars denote the positions of genes within these regions. Insets show PCR products for ligation products between *Hbb* and *Ahsp*, *Uros* or *P2ry6* on water (–), 3C or RNAPII-S5P ChIP-3C templates. (**d**) *Hbb* e4C microarray profiles for three ~2 Mb regions of genomic sequence in *trans* to *Hbb*, centered on *Slc4a1*, *Cd47* and *Fech*, showing the running mean enrichments of e4C signal over genomic signal for 100-kb windows.
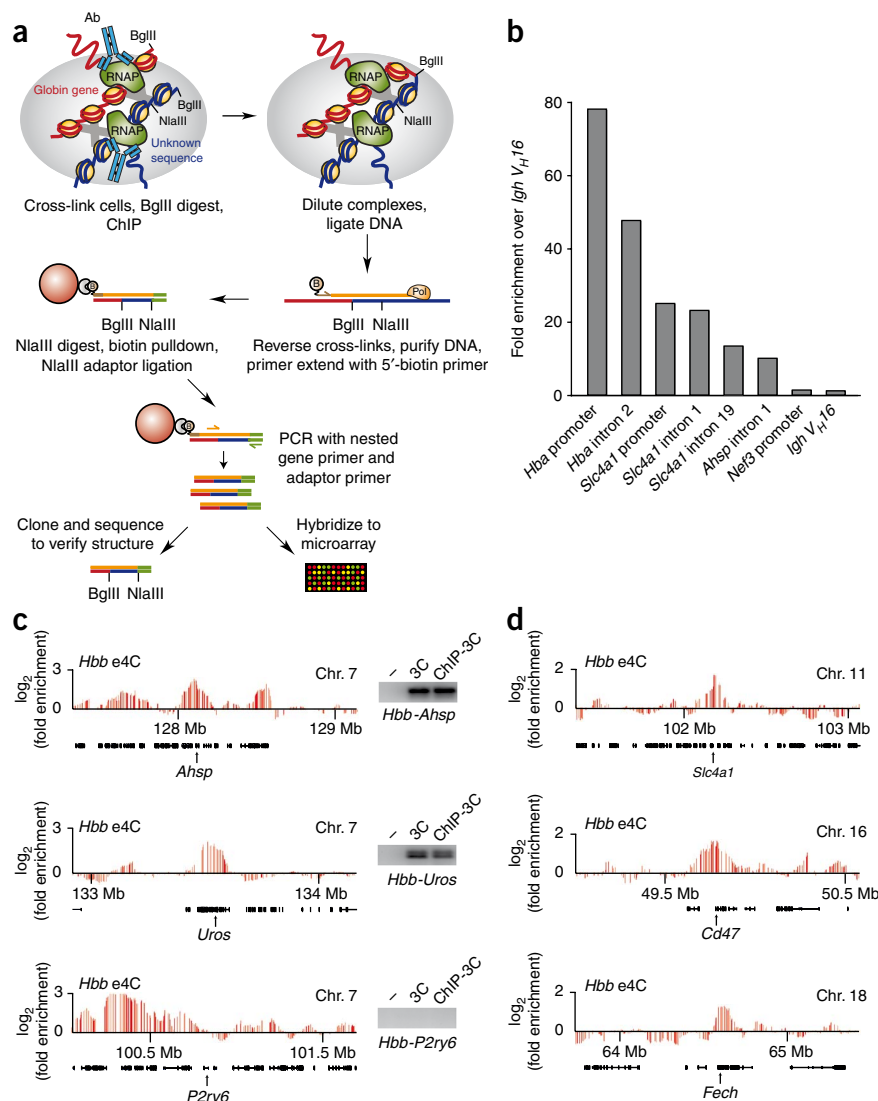
inactive *P2ry6* gene is negative by e4C (**Fig. 2c**). However, in contrast to a previous 4C study[28], the e4C results reveal extensive contacts between *Hbb* and selected genomic regions located on other chromosomes (examples shown in **Fig. 2d**). To identify the genomic regions that associate significantly with the globin genes, we used a sliding-window replicate Student's *t*-test to determine clusters of array probes that were enriched in e4C products. Notably, 88% of the clusters identified were located in *trans* to *Hbb* (241 of 273), implying that the majority of potential *Hbb* contacts in transcription factories occur with sequences on other chromosomes (**Supplementary Fig. 2** and **Supplementary Table 2**). We ruled out the possibility that random ligation between chromatin complexes could account for our results by mixing equal amounts of mouse and human chromatin before the RNAPII-S5P ChIP step (**Fig. 2a**) and then performing e4C with *Hbb* as bait (**Supplementary Note**). Sequencing the resultant e4C clones revealed that cross-ligation between mouse *Hbb* and human DNA was rare (1.3%; 1 of 77 clones) and could not account for the observed clustered-array hits.

We repeated the e4C assay with *Hba* as bait. The *Hba* e4C microarray data indicate that the locus associates with genomic regions located both in *cis* and in *trans* (**Supplementary Fig. 3**). The majority of *Hba* e4C clusters (93%; 514 of 551) were located on different chromosomes (**Supplementary Fig. 2** and **Supplementary Table 3**).

Taken together, our results imply that both mouse globin genes undergo extensive intra- and interchromosomal associations in transcription factories in erythroid cells.

To verify that e4C detects interactions between transcribing genes, we profiled erythroid RNAPII-S5P ChIP DNA by sequencing of paired end tags (ChIP-PETs)[29]. We used a conservative threshold to identify erythroid-transcribed genes and genomic regions with high confidence (**Supplementary Table 4**). As expected, most e4C clusters were centered on active genes; 80% of the *Hba* e4C clusters and 90% of the *Hbb* e4C clusters contained one or more annotated genes enriched in RNAPII-S5P (**Supplementary Fig. 4a**). Another 7% and 2%, respectively, of the e4C clusters contained regions of enriched RNAPII-S5P binding devoid of known genes, which may represent unannotated expressed genes or intergenic transcribed regions. Overall, the *Hbb* e4C clusters contained 724 active genes, and the *Hba* e4C clusters contained 1,286 active genes (**Supplementary Fig. 4b** and **Supplementary Note**).

## Preferential *Hba* and *Hbb* transcriptional networks

Because e4C includes an RNAPII-S5P ChIP enrichment step, one concern is that e4C simply detects associations between the globin genes and the most highly transcribed genes. Two lines of

Figure 3 Specificity of interchromosomal transcriptional networks. *Hba* (blue) and *Hbb* (red) e4C microarray profiles for ~2 Mb regions of genomic sequence in *trans* to both globin genes, showing the running mean enrichments of e4C signal over genomic signal for 100-kb windows. (**a**–**d**) Profiles are centered on genes identified by e4C as interacting with both *Hba* and *Hbb* (*Epb4.9*, *Xpo7* and *Spnb1*) (**a**), interacting with *Hba* (*Hnrpk* and *Pigq*) (**b**), interacting with *Hbb* (*Spna1* and *Fbxo9*) (**c**) and interacting with neither globin gene (*Gypa* and *B2m*) (**d**). Positions of genes and RNAPII-S5P ChIP-PET profiles (black) are shown below the e4C microarray profiles.

evidence argue against this possibility. First, e4C microarray profiles demonstrate that although some genes, such as *Spnb1*, *Epb4.9* and *Xpo7*, associate with both globin genes (**Fig. 3a**), other genes with comparable RNAPII-S5P occupancy preferentially associate with only one globin gene (for example, *Hnrpk*, *Pigq*, *Spna1* and *Fbxo9*; **Fig. 3b,c**) or with neither (for example, *B2m* and *Gypa*; **Fig. 3d**). These results indicate that co-associations detected by e4C are gene specific. In fact, 78% of the genes identified by e4C are unique to either *Hba* or *Hbb*, demonstrating that each locus associates preferentially with a specific subset or network of transcribed genes (**Supplementary Fig. 4b**). Second, although many highly transcribed genes associate with the globin genes, the majority of e4C hit genes are in the moderate to low range of RNAPII-S5P density (**Fig. 4a**). These results demonstrate that e4C is not solely identifying interactions between the most highly transcribed genes.

Finally, to validate the e4C results, we used the double-label RNA FISH data set described above (**Fig. 1d,e**). We reasoned that co-associating gene pairs detected by e4C should share transcription factories at higher frequencies. Indeed, we found that genes identified as

Hba or *Hbb* interacting partners by e4C colocalized with the globin genes at significantly higher frequencies ($P = 8 \times 10^{-5}$ for *Hba*, $P = 5 \times 10^{-4}$ for *Hbb*) than other genes (**Fig. 4b**). These results authenticate the e4C assay as a reliable indicator of genes that preferentially engage the same transcription factory. We conclude that the mouse globin genes preferentially associate with distinct but overlapping networks of transcribed genes.
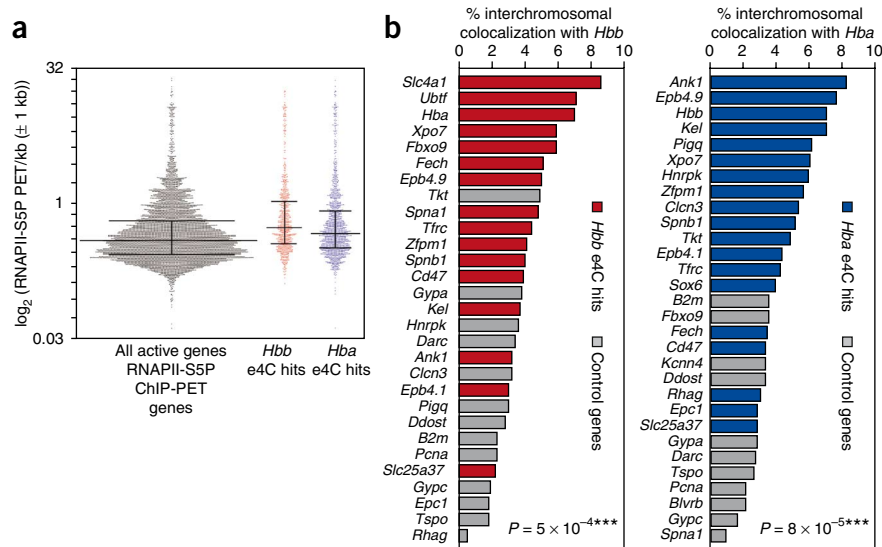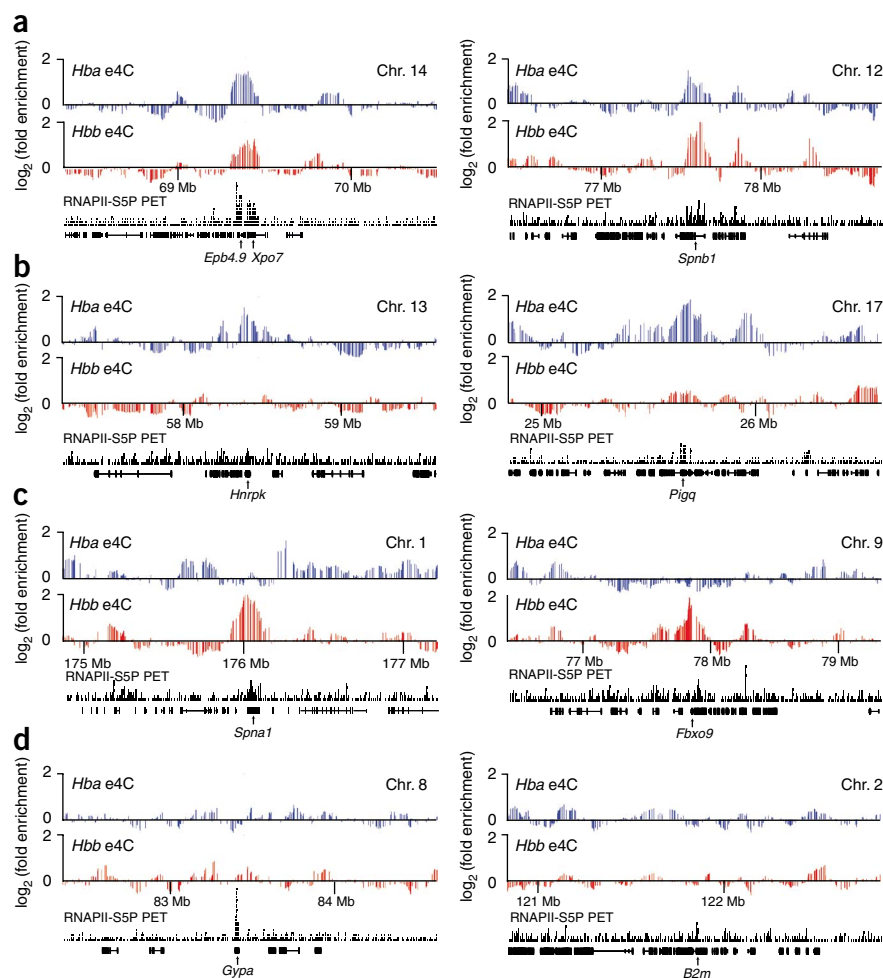
Co-association of specific gene triplets at transcription factories

Our e4C results indicate that each globin gene associates with hundreds of other genomic regions from nearly all mouse chromosomes

Figure 4 Validation of the e4C assay. (**a**) Scatter plot showing distributions of all erythroid-expressed genes (gray dots), *Hbb* e4C hits (red) and *Hba* e4C hits (blue), ranked by RNAPII-S5P PET density. Horizontal lines represent the median, 25th and 75th percentiles. (**b**) Validation of e4C by interchromosomal RNA FISH colocalization frequencies with *Hba* and *Hbb*. Genes identified by e4C as associating with *Hba* are highlighted in blue, *Hbb* e4C–associating genes are in red and non-hit genes in gray. *P* values are for differences in colocalization frequencies between e4C hit and non-hit genes.
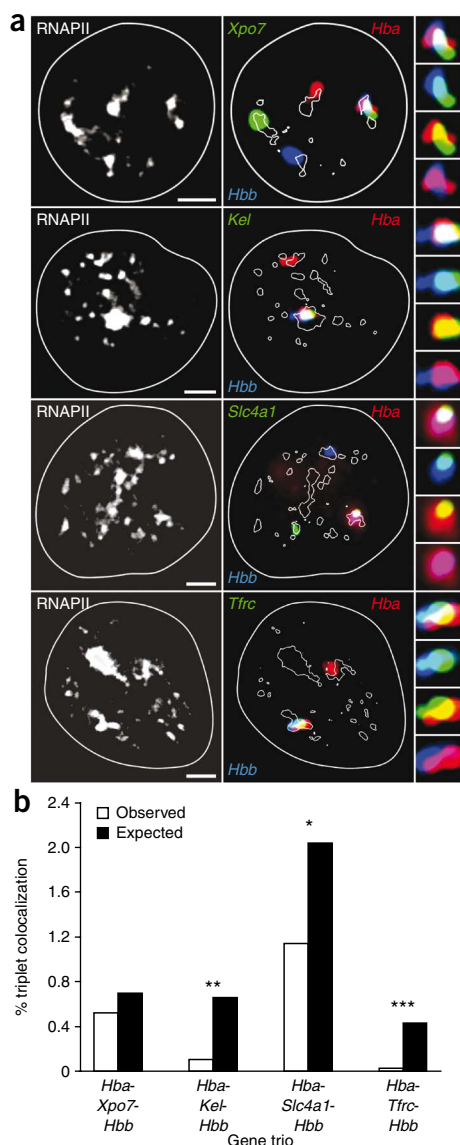
Figure 5 Co-association of three active genes within the same transcription factory. (**a**) Quadruple-label RNA immuno-FISH of three transcribed genes and RNAPII factories. RNAPII-S5P staining is shown in the panels on the left; RNA FISH signals in the same cells are shown in red (*Hba*), blue (*Hbb*) and green (top to bottom: *Xpo7*, *Kel*, *Slc4a1*, *Tfrc*) in the panels on the right. Side panels show enlarged images of the colocalizing FISH signals (top to bottom: triple label, blue and green, red and green, red and blue). Scale bar, 2 μm. (**b**) Bar chart showing the observed versus expected frequencies of gene triplet associations at a shared transcription factory. $*P < 0.05$; $**P < 0.005$; $***P < 0.001$.

and RNAPII transcription sites. We assayed *Hba*, *Hbb* and four other erythroid-expressed genes (*Kel*, *Slc4a1*, *Tfrc*, *Xpo7*) identified by e4C as interacting partners for both *Hba* and *Hbb*. We found multiple examples of three different gene transcription signals associated with the same RNAPII focus (**Fig. 5a**). Thus, a single transcription factory can indeed accommodate the simultaneous transcription of at least three genes, located on three different chromosomes.

We next scored the frequencies of simultaneous overlap between the three genes at the same RNAPII focus. Using the pairwise colocalization frequencies (**Supplementary Table 1**), we calculated expected triple-interaction frequencies, assuming independence between interacting gene pairs (**Supplementary Note**). For *Hba-Xpo7-Hbb*, we found that the observed frequency of triplet associations mirrored the expected frequencies (**Fig. 5b**). *Xpo7* seems to associate preferentially with *Hba* and *Hbb* independent of whether they are together or separate. In contrast, the *Hba-Kel-Hbb*, *Hba-Slc4a1-Hbb* and *Hba-Tfrc-Hbb* triplets occur at significantly lower-than-expected frequencies. These results suggest that *Kel*, *Slc4a1* and *Tfrc* preferentially colocalize with *Hbb* when it is not associated with *Hba*, and vice versa. These findings reveal a potential complex hierarchy of preferential associations within the transcription networks, which may represent mutually exclusive associations or physical constraints within the nucleus.

Globin transcription networks are enriched in Klf1-regulated genes
To understand the molecular basis for preferential associations in transcription factories, we searched the promoter sequences of e4C *Hba*- and *Hbb*-interacting genes for known transcription factor binding motifs. We found an enrichment of CACC motifs—potential binding sites for the erythroid-specific transcription factor Klf1[31] (Kruppel-like factor 1). Klf1 binds the *Hbb-b1* promoter[32], the *Hbb* locus control region (LCR)[32] and the *Hba* promoter and upstream enhancer region in erythroid cells[32,33]. *Hbb-b1* transcription is reduced by >80% in Klf1-deficient erythroid cells, whereas *Hba* transcription

(**Supplementary Fig. 2**). Previous estimates have suggested that a single transcription factory may be occupied by, on average, eight transcription units[30]. To address the question whether more than two genes could occupy the same factory, we performed quadruple-label RNA immuno-FISH to simultaneously visualize three active genes

Figure 6 Ectopic genes enter endogenous transcriptional networks. (**a**) Representative double-label RNA FISH for *HBB* transgenes (red) and endogenous *Hba* or *Hbb* genes (green) in definitive erythroid cells from transgenic lines (as indicated at top right of each panel), DAPI staining in blue. Scale bar, 2 μm. (**b**) Interchromosomal colocalization frequencies between *HBB* and *Hba* (blue bars) and *HBB* and *Hbb* (red bars) from six transgenic lines. Fold differences in transgene colocalization with *Hbb* versus *Hba* are shown along with the corresponding indicators of *P* values $*P < 0.05$; $**P < 0.005$; $***P < 0.001$.
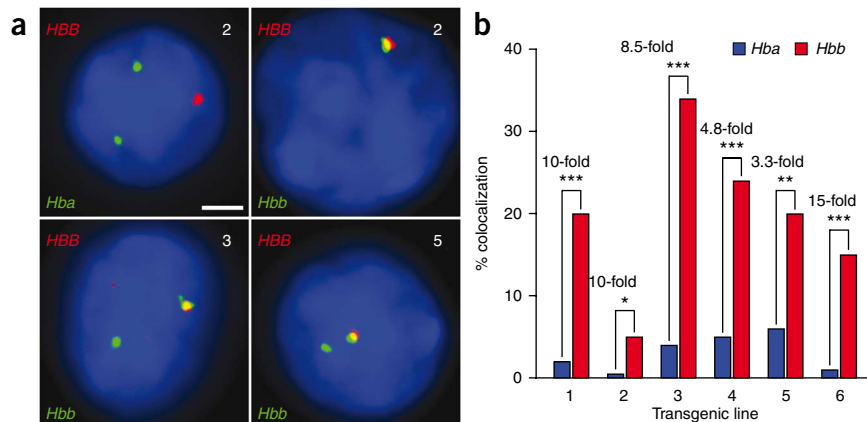
Figure 7 Co-regulated genes cluster in specialized transcription factories. (**a**) Immunofluorescence staining for Klf1 in definitive erythroid cells. Klf1 is shown in red, DAPI in blue. Note nonerythroid, Klf1-negative cell (bottom) demonstrating antibody specificity. Scale bar, 2 μm. (**b**) Immunofluorescence detection of Klf1 (red) and RNAPII-S5P (green) in definitive erythroid cells. Scale bar, 2 μm. (**c**) Double-label RNA immuno-FISH of nascent transcripts (green) and Klf1 foci (red). Side panels show enlarged images of selected nascent transcript signals with corresponding red channel (Klf1). Scale bar, 2 μm. (**d**) Graph showing proportions of RNA FISH signals found associated with Klf1 foci (black), or not associated with Klf1 foci (white). Green line shows 'background' association level of 20%, based on proportions of transcription factories containing high levels of Klf1. Indicators of P values are shown for Klf1 association frequencies higher than the background level (***$P < 0.001$). (**e**) Triple-label RNA immuno-FISH for pairs of nascent transcripts (blue and green, as indicated) and Klf1 foci (red). Side panels show enlarged images of the colocalizing FISH signals (top to bottom: triple label, blue and green, red and green, red and blue). Scale bar, 2 μm. (**f**) Graph showing proportions of colocalized pairs of RNA FISH signals found associated with Klf1 foci (black) or not associated with Klf1 foci (white). Green line shows 'background' association level of 20%, based on proportions of transcription factories containing high levels of Klf1. Indicators of P values are shown for increase in *Hbb-Cpox* Klf1 association frequency compared with *Cpox* Klf1 association frequency, and for decreases in globin-*Hist1h3f* Klf1 and globin-*Tubb5* Klf1 association frequencies compared to globin Klf1 association frequencies (**$P < 0.005$; ***$P < 0.001$).
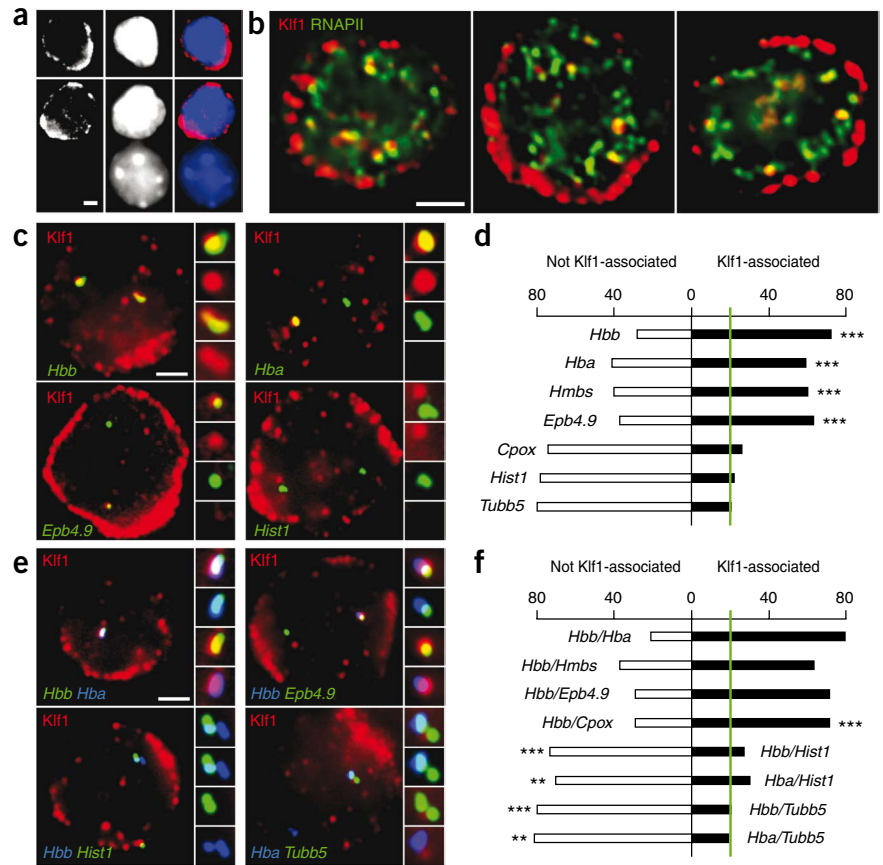
is less markedly affected[34,35]. We compiled a list of Klf1-regulated genes based on published expression profiles[36–38] (**Supplementary Table 5**). We found that genes upregulated by Klf1 were overrepresented among the *Hbb* e4C interacting genes ($P = 3 \times 10^{-8}$). *Hba* e4C interacting genes were also significantly overrepresented in genes upregulated by Klf1, but to a lesser extent ($P = 3 \times 10^{-4}$), perhaps reflecting *Hba*'s partial dependency on Klf1. In contrast, genes downregulated by Klf1 were not enriched ($P = 0.8$ for *Hba*, $P = 0.9$ for *Hbb*). These data suggest that genes upregulated by Klf1 preferentially share transcription factories and that shared regulatory factors may be the basis for transcription network specificity.

HBB transgenes relocate to the *Hbb* transcriptional interactome
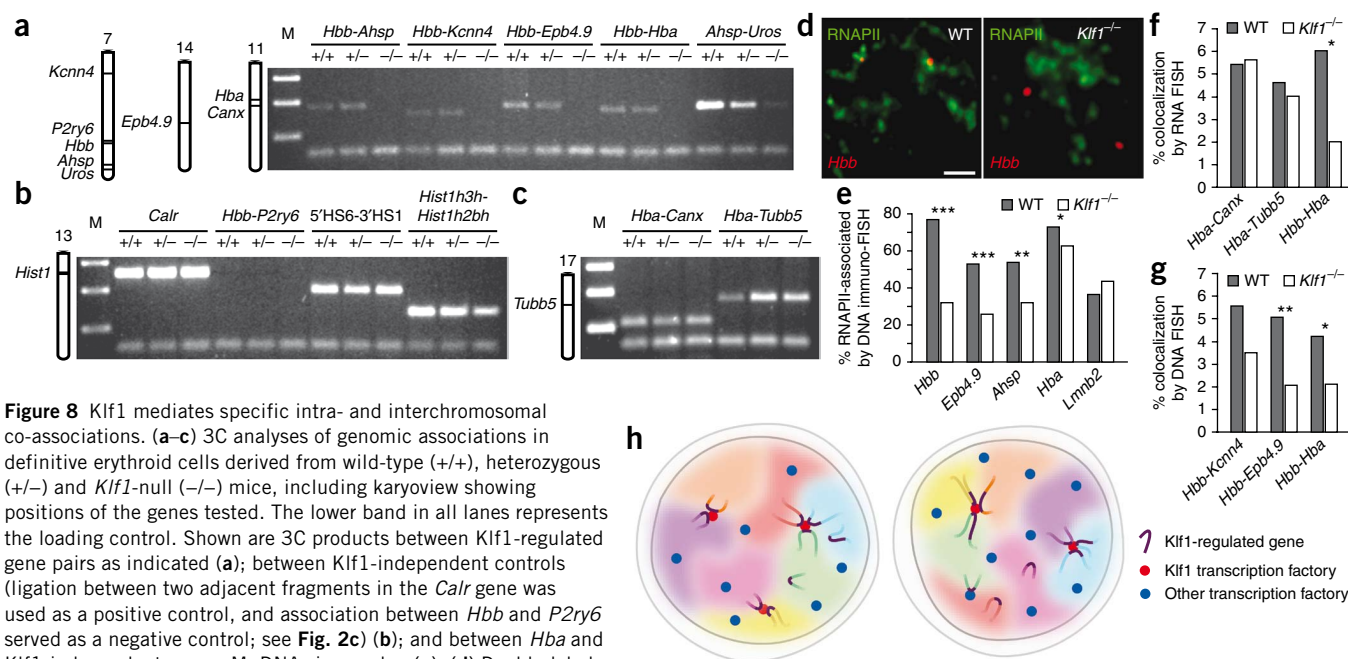
As a functional test of the theory that Klf1-regulated genes are preferentially organized in three-dimensional space to share factories, we investigated the subnuclear localization of Klf1-regulated transgenes relative to the endogenous *Hbb* and *Hba* genes. We chose the human β-globin (*HBB)* locus transgene, which is strongly dependent on Klf1 for transcription[39,40]. Two *HBB* transgenic lines contain large YACs encompassing the entire *HBB* locus, whereas four other lines contain a reporter gene driven by a fully functional microlocus LCR and *HBB* promoter[41]. We performed double-label RNA FISH to test whether the *HBB* transgenes could share transcription factories with the endogenous *Hbb* or *Hba* globin genes (**Fig. 6a**). Notably, the *HBB* transgene showed a strong preference for localizing to a factory occupied by *Hbb* as compared with *Hba* (**Fig. 6b**). This result cannot be explained

by physical linkage of the transgene to the *Hbb* locus, in that DNA FISH on metaphase spreads confirmed that none of the transgenes were integrated on chromosome 7 (data not shown). Colocalization frequencies between the transgene and endogenous *Hbb* locus were remarkably high (**Fig. 6b**), demonstrating that randomly integrated *HBB* transgenes have a strong preference for interchromosomal association with their co-regulated, endogenous counterparts in transcription factories. These data imply that the presence of a transcriptionally active transgene locus can spatially reorganize an ectopic chromosomal site to be near a co-regulated gene locus.

Specialized transcription factories

The above results imply that a subset of transcription factories may be specialized to preferentially transcribe a specific network of genes, such as Klf1-regulated genes. We therefore assessed the spatial distribution of Klf1 relative to RNAPII factories by immunofluorescence in mouse erythroid cells. In agreement with a recent study[42], we found that most Klf1 is located in the cytoplasm of mouse erythroid cells, whereas nuclear Klf1 is present in discrete sites (on average 40 foci per nucleus) (**Fig. 7a**). Nearly all Klf1 foci overlapped with RNAPII-S5P foci, indicating that 10–20% of transcription factories contain high levels of Klf1 (**Fig. 7b**).

We next assessed the position of several transcriptionally active, Klf1-regulated genes relative to Klf1 foci by RNA immuno-FISH (**Fig. 7c,d**). We found that the majority (59–72%) of actively transcribed alleles of *Hbb*, *Hba*, *Hmbs* and *Epb4.9* were preferentially

Figure 8 Klf1 mediates specific intra- and interchromosomal co-associations. (**a–c**) 3C analyses of genomic associations in definitive erythroid cells derived from wild-type (+/+), heterozygous (+/–) and *Klf1*-null (–/–) mice, including karyoview showing positions of the genes tested. The lower band in all lanes represents the loading control. Shown are 3C products between Klf1-regulated gene pairs as indicated (**a**); between Klf1-independent controls (ligation between two adjacent fragments in the *Calr* gene was used as a positive control, and association between *Hbb* and *P2ry6* served as a negative control; see **Fig. 2c**) (**b**); and between *Hba* and Klf1-independent genes. M, DNA size marker (**c**). (**d**) Double-label DNA immuno-FISH of *Hbb* (red) and RNAPII-S5P (green). WT, wild type. Scale bar, 2 μm. (**e**) Graph showing proportions of DNA FISH signals found associated with transcription factories in WT and *Klf1*$^{-/-}$ fetal liver cells, with the corresponding indicators of *P* values (*$P < 0.05$; **$P < 0.005$; ***$P < 0.001$). (**f**) Bar chart showing RNA FISH colocalization frequencies of the indicated gene pairs in WT and *Klf1*$^{-/-}$ cells. (**g**) Bar chart showing DNA FISH colocalization frequencies of the indicated gene pairs in WT and *Klf1*$^{-/-}$ cells. (**h**) Model of dynamic associations between genes in specialized transcription factories. Schematic representation of two cells that could represent the same cell at different times, or two cells with differing genome conformations within a population. Transcription factories are depicted as blue dots; Klf1-containing transcription factories are shown as red dots. Chromatin loops containing Klf1-regulated genes (aubergine segments) from the same or different chromosomes territories (colored areas) preferentially co-transcribe in the limited number of specialized Klf1-containing transcription factories. Temporarily nontranscribed alleles are positioned away from transcription factories. We propose that interactions between transcription network members are dynamic and may change over time, which may influence chromosomal conformations and chromosome positioning.

associated with 'Klf1 transcription factories'. In contrast, *Cpox*, which has only slightly decreased expression in the *Klf1* knockout[36], associated with Klf1 factories at only marginally higher frequencies (26%) than expected by a purely random distribution. Actively transcribed alleles of the Klf1-independent *Tubb5* and H2A/H2B histone genes (within the *Hist1h3f* (formerly *Hist1*) cluster on chromosome 13) showed no preferential localization to Klf1-containing factories (21% and 22%, respectively).

To test if Klf1 is involved in clustering Klf1-regulated genes, we assessed colocalizing pairs of genes relative to Klf1 foci (**Fig. 7e**). Using triple-label RNA immuno-FISH, we found that colocalizing pairs of Klf1-regulated genes are associated with Klf1 transcription factories at very high frequencies (63–79%; **Fig. 7f**). Notably, 71% of the *Cpox-Hbb* colocalizing pairs are associated with Klf1 foci, much higher than the frequency for *Cpox* alone ($P = 2 \times 10^{-4}$). This result clearly shows that *Cpox* alleles associate with *Hbb* preferentially in Klf1 factories. In contrast, colocalizing *Tubb5*-globin and histone-globin gene pairs show no preferential association with Klf1 transcription factories. This is significantly different from the percentage of globin alleles associating with Klf1 alone (*Hba*, $P = 1 \times 10^{-3}$ for *Tubb5* and $P = 2 \times 10^{-3}$ for histones; *Hbb*, $P = 1 \times 10^{-5}$ for *Tubb5* and $P = 4 \times 10^{-7}$ for histones) and shows that the vast majority of *Hbb* and *Hba* alleles that colocalize with *Tubb5* or *Hist1h3f* are not associated with Klf1 factories. Collectively, these data clearly show that transcribed, Klf1-regulated genes are preferentially located in transcription factories containing high levels of Klf1, and strongly suggest that these factories are shared by many other Klf1-regulated genes. Thus,

there are specialized transcription factories where active alleles of Klf1-regulated genes are more often found and are preferentially clustered with other Klf1-regulated genes.

Klf1 is required for clustering of Klf1-regulated genes

To test whether Klf1 is required for clustering of Klf1-regulated genes, we assessed intra- and interchromosomal associations in erythroid nuclei from wild-type and *Klf1*-knockout mice via 3C. Associations between *Hbb* and the Klf1-regulated genes *Ahsp* and *Kcnn4* were specifically disrupted in *Klf1*$^{-/-}$ erythroid cells but intact in *Klf1*$^{+/-}$ and wild type (**Fig. 8a**). Furthermore, interchromosomal associations between *Hbb* and *Epb4.9*, and between *Hbb* and *Hba*, were also disrupted specifically in the knockout. This effect is not limited to the *Hbb* locus, in that long-range associations between *Ahsp* and *Uros* were also decreased in *Klf1*$^{-/-}$ mice. In contrast, a known Klf1-independent interaction within the *Hbb* locus (LCR 5′HS6 and 3′HS1; ref. 43) was maintained in *Klf1*$^{-/-}$ mice (**Fig. 8b**), as was a long-range association between Klf1-independent histone genes (*Hist1h3h* and *Hist1h2bh*, separated by 1.8 megabases (Mb) on chromosome 13). Intra- and interchromosomal associations between *Hba* and the Klf1-independent *Canx* and *Tubb5* genes were also maintained in the knockout mice (**Fig. 8c**). These results show that interactions between Klf1-regulated genes are specifically disrupted in the absence of Klf1.

Because our data support the concept that associations between active genes occur in transcription factories, we asked whether key Klf1-regulated genes show reduced factory occupancy in *Klf1*$^{-/-}$ erythroid cells. Indeed, *Hbb*, *Epb4.9* and *Ahsp* all show markedly reduced association with transcription factories in *Klf1*$^{-/-}$ erythroid

cells, consistent with their high dependence on Klf1 (**Fig. 8d,e**). In contrast, the percentage of *Hba* alleles associated with factories was only mildly decreased, possibly reflecting *Hba*'s partial dependence on Klf1. Factory occupancy of the Klf1-independent *Lmnb2* gene was unchanged. Thus, Klf1-regulated genes show reduced association with transcription factories in the absence of Klf1, which may in part explain their reduced expression[36–38].

We confirmed by RNA FISH that the number of active *Hbb* alleles was markedly reduced in *Klf1*^{−/−} erythroid cells (to 5% that in wild-type cells). Notably, those *Hbb* alleles that were still active in *Klf1*^{−/−} erythroid cells showed markedly reduced association with *Hba* (**Fig. 8f**). In contrast, colocalization frequencies between *Hba*, *Canx* and *Tubb5* pairs were unchanged in the knockout (**Fig. 8f**), in agreement with the 3C results (**Fig. 8c**). Thus, the partially Klf1-dependent *Hba* maintains associations with Klf1-independent genes, whereas its association with the highly Klf1-dependent *Hbb* gene is specifically disrupted. We noted that RNA FISH signals for *Hbb* were considerably weaker in the knockout, suggesting a reduced rate of transcriptional firing or elongation. This precluded RNA FISH analyses of other Klf1-regulated genes with considerably lower transcription rates than *Hbb*. We therefore used DNA FISH to determine changes in colocalization frequencies between *Hbb*, *Epb4.9* and *Kcnn4* pairs. We found that intrachromosomal (*Hbb-Kcnn4*) and interchromosomal (*Hbb-Hba*; *Hbb-Epb4.9*) interaction frequencies were reduced in *Klf1*^{−/−} cells (**Fig. 8g**). Collectively, these results clearly demonstrate that Klf1 is required for preferential colocalization of Klf1-regulated genes at shared transcription factories.

DISCUSSION

Using a combination of techniques (e4C, 3C, RNA FISH, DNA FISH and immuno-FISH), we have shown that the mouse globin genes preferentially associate with hundreds of other transcribed genomic loci in transcription factories. The globin-interacting genes are distributed over nearly all mouse chromosomes, uncovering extensive intra- and interchromosomal transcriptional interaction networks in erythroid nuclei. It is highly unlikely that all of these interactions occur simultaneously in the same cell. Instead, our data on gene triplet associations at factories imply that genome organization is inherently plastic. We propose that multiple different genome conformations exist and that each brings the globin genes into close proximity with a varied subset of their preferred transcriptional partners (**Fig. 8h**). Although gene associations at factories seem to be dynamic[44], it is presently not known whether these whole-genome conformations are dynamically interchangeable within one nucleus or whether individual conformations are relatively stable in a subset of nuclei.

Within the globin transcriptional networks, Klf1-regulated genes are preferentially transcribed at a limited number of specialized transcription factories containing large amounts of Klf1. Our data also show that Klf1-regulated genes share Klf1-containing factories and that Klf1 is required for clustering of these co-regulated genes. It is important to point out that the majority of Klf1-regulated genes are not dependent on Klf1 for expression but instead require Klf1 for increased expression in the definitive erythroid lineage. For example, many of the genes encoding proteins involved in iron uptake and heme synthesis are ubiquitously expressed in all cell types but are highly upregulated by Klf1 during erythropoiesis[36,37]. We propose that specialized transcription factories boost the expression of clustered, co-regulated genes by concentrating specific transcription factors required for their coordinate or increased transcription (**Fig. 8h**). This may occur through a self-organization process

whereby locally elevated concentrations of transcription factors and their cognate binding sites increase the probability of gene re-initiation, thus increasing occupancy time and transcriptional output at a shared factory. Such a model does not propose that specific pairwise interactions of genes are essential for their expression, but rather that individual genes may indirectly benefit from cooperative associations in these specialized microenvironments. Consequently, removal of a member of the network would not be expected to affect transcription of other network members to any great extent. In agreement with this, transcription and expression of several genes that associate with *Hbb* did not change in *Hbb* LCR knockout mice (data not shown), in which *Hbb* factory association and expression are markedly reduced[15].

The concept of transcription factor–mediated spatial genome organization is supported by the observation that ectopic Klf1-regulated transgenes enter the same transcription sites as a co-regulated endogenous gene. This finding implies that transcriptional associations may considerably influence genome organization. This is supported indirectly by observed alterations in chromosomal co-associations when transcription is inhibited[5,13]. Thus, we propose that preferential associations in transcription factories substantially affect higher order chromosomal conformations and are a major driving force in tissue-specific chromosome positioning[45].

Our results contrast with previous subgenomic 4C studies that detected few interchromosomal contacts for *Hbb* and concluded that active *Hbb* loci interact primarily in *cis*[28], regardless of transcription[46]. We propose that the reasons for this discrepancy are probably the increased sensitivity and specificity of e4C. The biotin pre-enrichment step removes the thousands of copies of genomic DNA in the PCR reaction, which contribute to the probe in other 4C assays, potentially causing background noise upon microarray hybridization. In addition, the RNAPII-S5P ChIP step specifically enriches for transcriptionally active alleles, thus focusing on interactions at transcription factories and excluding cells not transcribing the bait gene. Conventional 3C and 4C approaches inherently average the interactions of all alleles in a population, active and temporarily nontranscribed; thus, preferential associations among the transcribed subpopulation of alleles might escape detection with these techniques.

Previous studies have focused on small numbers of genes or genetic elements that functionally cluster in three dimensions, such as nucleolar rDNA repeats[47], tRNA genes in yeast[48], silenced *Hox* genes in *Drosophila*[49], virally induced associations between the interferon-β gene and NF-κB–bound sites[6], between EZH2-bound sites[50], and clustering of transiently transfected reporter constructs[51]. Here we used a genome-wide e4C screen to identify extensive spatial networks of active genes, demonstrating that interchromosomal clustering of genes is a widespread principle of nuclear organization.

Our results imply that transcriptional regulation should be considered in the context of the three-dimensional organization of the genome rather than as a mechanism that acts on single genes in isolation. Co-regulated genes cluster in nuclear space and potentially collaborate to create transcription sites that are optimized for their regulated expression. Thus, the concept of regulation of cell-type gene expression patterns by combinatorial transcription factor control is played out in the nucleus as combinatorial associations between multiple genes at specialized transcription sites, creating functional overlapping transcription networks.

METHODS

Methods and any associated references are available in the online version of the paper at http://www.nature.com/naturegenetics/.

1. Lanctôt, C., Cheutin, T., Cremer, M., Cavalli, G. & Cremer, T. Dynamic genome architecture in the nuclear space: regulation of gene expression in three dimensions. *Nat. Rev. Genet.* **8**, 104–115 (2007).
2. Bolzer, A. *et al.* Three-dimensional maps of all chromosomes in human male fibroblast nuclei and prometaphase rosettes. *PLoS Biol.* **3**, e157 (2005).
3. Chambeyron, S. & Bickmore, W.A. Chromatin decondensation and nuclear reorganization of the HoxB locus upon induction of transcription. *Genes Dev.* **18**, 1119–1130 (2004).
4. Volpi, E.V. *et al.* Large-scale chromatin organization of the major histocompatibility complex and other regions of human chromosome 6 and its response to interferon in interphase nuclei. *J. Cell Sci.* **113**, 1565–1576 (2000).
5. Branco, M.R. & Pombo, A. Intermingling of chromosome territories in interphase suggests role in translocations and transcription-dependent associations. *PLoS Biol.* **4**, e138 (2006).
6. Apostolou, E. & Thanos, D. Virus infection induces NF-κB-dependent interchromosomal associations mediating monoallelic IFN-β gene expression. *Cell* **134**, 85–96 (2008).
7. Spilianakis, C.G., Lalioti, M.D., Town, T., Lee, G.R. & Flavell, R.A. Interchromosomal associations between alternatively expressed loci. *Nature* **435**, 637–645 (2005).
8. Zhao, Z. *et al.* Circular chromosome conformation capture (4C) uncovers extensive networks of epigenetically regulated intra- and interchromosomal interactions. *Nat. Genet.* **38**, 1341–1347 (2006).
9. Brown, K.E., Baxter, J., Graf, D., Merkenschlager, M. & Fisher, A.G. Dynamic repositioning of genes in the nucleus of lymphocytes preparing for cell division. *Mol. Cell* **3**, 207–217 (1999).
10. Osborne, C.S. *et al.* Myc dynamically and preferentially relocates to a transcription factory occupied by *Igh. PLoS Biol.* **5**, e192 (2007).
11. Sexton, T., Schober, H., Fraser, P. & Gasser, S.M. Gene regulation through nuclear organization. *Nat. Struct. Mol. Biol.* **14**, 1049–1055 (2007).
12. Jackson, D.A., Hassan, A.B., Errington, R.J. & Cook, P.R. Visualization of focal sites of transcription within human nuclei. *EMBO J.* **12**, 1059–1065 (1993).
13. Mitchell, J.A. & Fraser, P. Transcription factories are nuclear subcompartments that remain in the absence of transcription. *Genes Dev.* **22**, 20–25 (2008).
14. Osborne, C.S. *et al.* Active genes dynamically colocalize to shared sites of ongoing transcription. *Nat. Genet.* **36**, 1065–1071 (2004).
15. Ragoczy, T., Bender, M.A., Telling, A., Byron, R. & Groudine, M. The locus control region is required for association of the murine β-globin locus with engaged transcription factories during erythroid maturation. *Genes Dev.* **20**, 1447–1457 (2006).
16. Wansink, D.G. *et al.* Fluorescent labeling of nascent RNA reveals transcription by RNA polymerase II in domains scattered throughout the nucleus. *J. Cell Biol.* **122**, 283–293 (1993).
17. Iborra, F.J., Pombo, A., Jackson, D.A. & Cook, P.R. Active RNA polymerases are localized within discrete transcription "factories" in human nuclei. *J. Cell Sci.* **109**, 1427–1436 (1996).
18. Chubb, J.R., Trcek, T., Shenoy, S.M. & Singer, R.H. Transcriptional pulsing of a developmental gene. *Curr. Biol.* **16**, 1018–1025 (2006).
19. Levsky, J.M., Shenoy, S.M., Pezo, R.C. & Singer, R.H. Single-cell gene expression profiling. *Science* **297**, 836–840 (2002).
20. Raj, A., Peskin, C.S., Tranchina, D., Vargas, D.Y. & Tyagi, S. Stochastic mRNA synthesis in mammalian cells. *PLoS Biol.* **4**, e309 (2006).
21. Dekker, J., Rippe, K., Dekker, M. & Kleckner, N. Capturing chromosome conformation. *Science* **295**, 1306–1311 (2002).
22. Brown, J.M. *et al.* Association between active genes occurs at nuclear speckles and is modulated by chromatin environment. *J. Cell Biol.* **182**, 1083–1097 (2008).
23. Brown, J.M. *et al.* Coregulated human globin genes are frequently in spatial proximity when active. *J. Cell Biol.* **172**, 177–187 (2006).
24. Hu, Q. *et al.* Enhancing nuclear receptor-induced transcription requires nuclear motor and LSD1-dependent gene networking in interchromatin granules. *Proc. Natl. Acad. Sci. USA* **105**, 19199–19204 (2008).
25. Smith, K.P., Moen, P.T., Wydner, K.L., Coleman, J.R. & Lawrence, J.B. Processing of endogenous pre-mRNAs in association with SC35 domains is gene specific. *J. Cell Biol.* **144**, 617–629 (1999).
26. Xing, Y., Johnson, C.V., Moen, P.T. Jr., McNeil, J.A. & Lawrence, J. Nonrandom gene organization: structural arrangements of specific pre-mRNA transcription and splicing with SC35 domains. *J. Cell Biol.* **131**, 1635–1647 (1995).
27. Phatnani, H.P. & Greenleaf, A.L. Phosphorylation and functions of the RNA polymerase II CTD. *Genes Dev.* **20**, 2922–2936 (2006).
28. Simonis, M. *et al.* Nuclear organization of active and inactive chromatin domains uncovered by chromosome conformation capture-on-chip (4C). *Nat. Genet.* **38**, 1348–1354 (2006).
29. Wei, C.L. *et al.* A global map of p53 transcription-factor binding sites in the human genome. *Cell* **124**, 207–219 (2006).
30. Pombo, A. *et al.* Regional specialization in human nuclei: visualization of discrete sites of transcription by RNA polymerase III. *EMBO J.* **18**, 2241–2253 (1999).
31. Miller, I.J. & Bieker, J.J. A novel, erythroid cell-specific murine transcription factor that binds to the CACCC element and is related to the Kruppel family of nuclear proteins. *Mol. Cell. Biol.* **13**, 2776–2786 (1993).
32. Shyu, Y.C. *et al.* Chromatin-binding *in vivo* of the erythroid Kruppel-like factor, EKLF, in the murine globin loci. *Cell Res.* **16**, 347–355 (2006).
33. Vernimmen, D., De Gobbi, M., Sloane-Stanley, J.A., Wood, W.G. & Higgs, D.R. Long-range chromosomal interactions regulate the timing of the transition between poised and active gene expression. *EMBO J.* **26**, 2041–2051 (2007).
34. Nuez, B., Michalovich, D., Bygrave, A., Ploemacher, R. & Grosveld, F. Defective haematopoiesis in fetal liver resulting from inactivation of the EKLF gene. *Nature* **375**, 316–318 (1995).
35. Perkins, A.C., Sharpe, A.H. & Orkin, S.H. Lethal β-thalassaemia in mice lacking the erythroid CACCC-transcription factor EKLF. *Nature* **375**, 318–322 (1995).
36. Drissen, R. *et al.* The erythroid phenotype of EKLF-null mice: defects in hemoglobin metabolism and membrane stability. *Mol. Cell. Biol.* **25**, 5205–5214 (2005).
37. Hodge, D. *et al.* A global role for EKLF in definitive and primitive erythropoiesis. *Blood* **107**, 3359–3370 (2006).
38. Nilson, D.G., Sabatino, D.E., Bodine, D.M. & Gallagher, P.G. Major erythrocyte membrane protein genes in EKLF-deficient mice. *Exp. Hematol.* **34**, 705–712 (2006).
39. Perkins, A.C., Gaensler, K.M. & Orkin, S.H. Silencing of human fetal globin expression is impaired in the absence of the adult β-globin gene activator protein EKLF. *Proc. Natl. Acad. Sci. USA* **93**, 12267–12271 (1996).
40. Wijgerde, M. *et al.* The role of EKLF in human β-globin gene competition. *Genes Dev.* **10**, 2894–2902 (1996).
41. Talbot, D. *et al.* A dominant control region from the human β-globin gene locus conferring integration site-independent gene expression. *Nature* **338**, 352–355 (1989).
42. Quadrini, K.J., Gruzglin, E. & Bieker, J.J. Non-random subcellular distribution of variant EKLF in erythroid cells. *Exp. Cell Res.* **314**, 1595–1604 (2008).
43. Drissen, R. *et al.* The active spatial organization of the β-globin locus requires the transcription factor EKLF. *Genes Dev.* **18**, 2485–2490 (2004).
44. Fraser, P. & Bickmore, W. Nuclear organization of the genome and the potential for gene regulation. *Nature* **447**, 413–417 (2007).
45. Parada, L.A., McQueen, P.G. & Misteli, T. Tissue-specific spatial organization of genomes. *Genome Biol.* **5**, R44 (2004).
46. Palstra, R.J. *et al.* Maintenance of long-range DNA interactions after inhibition of ongoing RNA polymerase II transcription. *PLoS One* **3**, e1661 (2008).
47. Scheer, U. & Hock, R. Structure and function of the nucleolus. *Curr. Opin. Cell Biol.* **11**, 385–390 (1999).
48. Thompson, M., Haeusler, R.A., Good, P.D. & Engelke, D.R. Nucleolar clustering of dispersed tRNA genes. *Science* **302**, 1399–1401 (2003).
49. Grimaud, C. *et al.* RNAi components are required for nuclear clustering of Polycomb group response elements. *Cell* **124**, 957–971 (2006).
50. Tiwari, V.K., Cope, L., McGarvey, K.M., Ohm, J.E. & Baylin, S.B. A novel 6C assay uncovers Polycomb-mediated higher order chromatin conformations. *Genome Res.* **18**, 1171–1179 (2008).
51. Xu, M. & Cook, P.R. Similar active genes cluster in specialized transcription factories. *J. Cell Biol.* **181**, 615–623 (2008).

ONLINE METHODS

Immunofluorescence. RNAPII-S5P was detected with monoclonal antibody CTD4H8 (Upstate) and visualized with appropriately labeled secondary antibodies or by direct labeling with Alexa Fluor 594–Fab fragments (Zenon labeling kit; Invitrogen). Sc35 was detected with antibody S4045 (Sigma). Klf1 was detected with a mouse monoclonal antibody 6B3(N) (ref. 42) followed by a FITC-labeled goat secondary antibody to mouse (Jackson ImmunoResearch) or successive layers of biotinylated goat antibody to mouse (Jackson ImmunoResearch) and Alexa Fluor-647–conjugated streptavidin (Invitrogen).

Immunofluorescence was carried out on cells fixed in formaldehyde or formaldehyde–acetic acid. Image stacks were collected and subjected to iterative restoration using Volocity image analysis software.

RNA FISH and RNA immuno-FISH. RNA FISH was performed as described[14]. A minimum of 200 loci were scored to determine the colocalization frequency for each gene pair.

For RNA immuno-FISH, proteins were detected by applying the appropriate antibodies following RNA FISH signal detection. For Sc35 RNA immuno-FISH, erythroid cells were fixed first for 3 min in PBS–4% formaldehyde and then for 15 min as in RNA FISH[14]. CTD4H8 anti-RNAPII was visualized with Alexa Fluor-350, combined with FITC, Texas Red and Cy5 detection of RNA. 6B3(N) antibody to Klf1 was detected with Alexa Fluor 647, and RNA signals were visualized by using secondary antibodies conjugated to Rhodamine RX and FITC (Jackson ImmunoResearch).

DNA FISH and DNA immuno-FISH. BAC clones (BACPAC Resources) labeled by nick translation were used for DNA FISH as described[52] with modifications (data not shown). Fetal liver cells (embryonic day 13.5) were fixed as for RNA FISH[14].

3C. 3C was performed as described[53]. As loading control, a 50-base-pair duplex oligonucleotide was added to the 3C material before aliquoting and PCR amplification.

e4C. Cells were fixed as for 3C (ref. 53), with fixation for 5 min and digestion with BglII. Nuclear debris was removed by centrifugation of 100-µg aliquots of chromatin in 1 ml ChIP buffer (16.7 mM Tris-HCl pH 8, 167 mM NaCl, 1.2 mM EDTA, 1.1% Triton X-100, 0.01% SDS, protease inhibitors (Roche Complete, EDTA-free)), before immunoprecipitation with antibody to RNAPII-S5P (Ab5131; Abcam), adsorbed to protein A–bound magnetic beads (Dynabeads; Invitrogen). Bound chromatin was washed three times with 20 mM Tris-HCl pH 8, 150 mM NaCl, 2 mM EDTA, 1% Triton X-100, 0.1% SDS, protease inhibitors, then three times with the same buffer with 500 mM NaCl, and finally three times with 10 mM Tris-HCl pH 8, 1 mM EDTA, before elution at 65 °C with 50 µl NEB3 buffer (New England Biolabs) and 1.6% SDS for 30 min. Chromatin was diluted to 1 ml with ligation buffer, treated with 1% Triton X-100 and ligated, and the DNA was purified as for conventional 3C. Twelve to fifteen aliquots (100 ng DNA each) were used for primer extension with Vent (exo⁻) DNA polymerase (New England Biolabs) and 100 nM biotinylated bait-specific primer in 50-µl reactions. After digestion with NlaIII, excess primer was removed on spin columns (Qiagen). Biotinylated products were bound to streptavidin-coated magnetic beads (Dynabeads M-280; Invitrogen) and unbound products removed by the kilobaseBINDER kit (Invitrogen), before an additional digestion with NlaIII. Beads were washed with the kilobaseBINDER wash buffer, and 5 µM adaptor was ligated with T4 DNA ligase in 40-µl reactions. The beads were washed again, before amplification of e4C products by PCR with hot-start *Taq* polymerase (HotStar; Qiagen) and 400 nM each nested bait-specific primer and adaptor-specific primer in 50-µl reactions. PCR conditions: 95 °C, 15 min; 35 cycles of 94 °C, 30 s, 55 °C, 30 s, 72 °C, 1 min; 72 °C, 10 min. Primer sequences are available on request.

Microarrays. e4C material was labeled and competitively hybridized with digested mouse genomic DNA (as for standard ChIP-on-chip procedures; NimbleGen Systems) to a custom NimbleGen array (384,522 isothermal 45- to 65-mer probes mapping to nonrepetitive BglII-NlaIII fragments of suitable size from the mouse genome (NCBI m36)).

Hybridization signals were globally normalized and mapped to genomic position. Three biological replicates were performed for each e4C experiment, and the normalized signals were averaged. Clusters of e4C hits were determined by running a two-tailed windowed replicate *t*-test (250-kb sliding window; *P*-value cutoff of 0.01 after Benjamini-Hochberg false discovery rate correction) on probes with e4C signal >4-fold above genomic control.

RNAII-S5P ChIP PET. RNAPII-S5P ChIP was performed on erythroid cells as described for e4C, with the following exceptions. (i) Instead of digestion, nuclei were resuspended in sonication buffer (50 mM Tris-HCl pH 8, 10 mM EDTA, 1% SDS, protease inhibitors (Roche)), and chromatin was sonicated to an average length of <1 kb. (ii) Chromatin was eluted from protein A beads by incubation at 50 °C for 30 min with 1% SDS, 100 mM NaHCO₃. ChIP DNA was purified and converted to PETs for sequencing as described[29]. Erythroid-expressed genes were defined as those containing a cluster of three or more overlapping PETs. PET densities were calculated by dividing the numbers of PETs within the gene (±1 kb), by the gene size in kilobases. An erythroid-expressed gene was classed as an e4C hit with *Hba* or *Hbb* if the gene or its flanking sequences (±10 kb) contributed to a significant e4C cluster.

Transgenic mouse lines. Transgenic lines 1 and 2 contain 150-kb (ref. 54) and 248-kb (respectively) human *HBB* locus YACs. Lines 3–6 contain a plasmid construct with the *HBB* LCR (hypersensitive sites 1–4)[41] and *HBB* promoter driving a reporter gene.

Statistical analyses. RNA FISH colocalization frequencies between pairs of transcripts were compared by two-tailed Fisher's exact tests. RNA FISH colocalization frequencies with the globin transcripts were compared between e4C hit genes and non-hitting genes by two-tailed *t*-tests, after normality of the distributions were confirmed by Kolmogorov-Smirnov tests. For promoter motif analysis, a kilobase of sequence upstream of all active erythroid genes was extracted by Ensembl BioMart, and the frequency of binding motifs, scored using an 80% match threshold against the positional weight matrix from the JASPAR database[55], counted with the TFBS package[56]. Motif frequencies were compared between e4C hit genes and other active genes by *t*-tests with Bonferroni multiple-testing corrections. Overrepresentation of Klf1-regulated genes among e4C hits, assuming independence of the two variables, was calculated from the hypergeometric probability distribution. Comparisons of Klf1 association frequencies with the 'background' frequency of 20% were made by two-tailed Fisher's exact tests. Fisher's exact tests were used to compare the Klf1 association frequencies between colocalized RNA FISH signals and individual RNA FISH signals.

URLs. GEO, http://www.ncbi.nlm.nih.gov/geo/; ArrayExpress, http://www.ebi.ac.uk/microarray-as/ae/.

52. Cremer, M. *et al.* Multicolor 3D fluorescence *in situ* hybridization for imaging interphase chromosomes. in *Methods in Molecular Biology* (ed. R. Hancock) 205–239 (Humana Press, New York, 2008).
53. Cope, N.F. & Fraser, P. Chromosome conformation capture. *CSH Protoc.* published online; doi:10.1101/pdb.prot5137 (2009).
54. Tanimoto, K., Liu, Q., Bungert, J. & Engel, J.D. Effects of altered gene order or orientation of the locus control region on human beta-globin gene expression in mice. *Nature* **398**, 344–348 (1999).
55. Sandelin, A., Alkema, W., Engstrom, P., Wasserman, W.W. & Lenhard, B. JASPAR: an open-access database for eukaryotic transcription factor binding profiles. *Nucleic Acids Res.* **32**, D91–D94 (2004).
56. Lenhard, B. & Wasserman, W.W. TFBS: computational framework for transcription factor binding site analysis. *Bioinformatics* **18**, 1135–1136 (2002).